

Vibrational Recognition of Hydrogen-Bonded Water Networks on a Metal Surface

Sheng Meng,^{1,2} L. F. Xu,¹ E. G. Wang,¹ and Shiwu Gao²

¹*Institute of Physics, Chinese Academy of Sciences, P.O. Box 603, Beijing, 100080, China*

²*Department of Applied Physics, Chalmers University of Technology and Göteborg University, SE-412 96 Göteborg, Sweden*

(Received 4 June 2002; published 7 October 2002)

The adsorption of water on Pt(111) surface has been studied with *ab initio* molecular dynamics simulation. Both the energetics and vibrational dynamics indicate the existence of a well-ordered molecular bilayer on this surface. This conclusion is in contrast to the recent result of water on Ru(0001) surface, but agrees with available experiments. In addition, our calculation identifies two different hydrogen bonds in the bilayer. Both can be directly recognized from the vibrational spectra of the OH stretch modes.

DOI: 10.1103/PhysRevLett.89.176104

PACS numbers: 68.43.Bc, 68.35.-p, 82.30.Rs

Water adsorption on single crystalline surfaces of solids has been intensively investigated both experimentally [1] and theoretically [2] during the past few decades. On a number of metal surfaces, deposition of water usually leads to well-ordered structures such as one-dimensional (1D) chain [3], bilayer, and islands and clusters [4,5], before bulk ice is formed. Among these structures, water bilayer with a $\sqrt{3} \times \sqrt{3}$ hexagonal pattern at $2/3$ monolayer coverage, is mostly interesting because it marks the initial stage of formation of the 2D ice, the hydrogen-bonded network. Such a bilayer structure has been proposed and/or observed on several metal surfaces including Ru(0001), Pt(111), and Rh(111), and seems to be a general feature of the 2D water network. However, recent study by Feibelman for water/Ru(0001) [6] has ruled out the existence of the molecular bilayer, as usually accepted by the community. Instead it was found that the waters in the bilayer were partially dissociated, with one OH bond broken. Whether this conclusion is specific to Ru or general to other systems is unclear. Besides, how a metal substrate affects the structure and the interaction in the bilayer remains to be an important issue that needs to be investigated.

In this Letter, we present a computational study of submonolayer water on Pt(111) using *ab initio* molecular dynamics simulations based on density functional theory (DFT). In contrast to Feibelman's findings on Ru(0001), we found that the molecular bilayer on the Pt(111) surface is energetically favored and stable. Besides, the vibrational spectra of all characteristic modes of the bilayer have been identified and correspond one-by-one to the measured data obtained from high-resolution electron energy loss spectroscopy (HREELS) and helium atom scattering. We also found that the hydrogen bond (H bond) in the bilayer are of two types: a strong H bond in the top layer and two weak H bonds in the bottom layer, due to different interaction with the substrate. We further demonstrate that the OH stretch in the bilayer, which is sensitive to the H-bond formation and structural transformation, may provide a general way for recognition of

adsorbed waters and other hydrogen-bonded species at interfaces.

The first-principle calculation has been performed using the Vienna *ab initio* simulation program, VASP [7]. A four-layer slab, separated by a vacuum layer of 13 Å, is used to model the Pt(111) surface (with the calculated lattice constant of 3.99 Å). Water molecules were put on one side of the slab. Two supercells, a $p(3 \times 3)$ for monomer and dimer adsorption and a $\sqrt{3} \times \sqrt{3}R30^\circ$ for the bilayer, have been calculated. The Monkhorst-Pack scheme [8] with $3 \times 3 \times 1$ and $5 \times 5 \times 1$ k points has been used for integration in the surface Brillouin zone for the two supercells, respectively. Energy cut off for the plane waves is 300 eV. Fermi level is smeared by the Gaussian method [9] with a width of 0.2 eV. This set of parameters assures a total energy convergence of 0.01 eV per atom. In structure search, the molecules and the first layer Pt atoms are relaxed simultaneously. The search is stopped when forces on all relaxed atoms are less than 0.03 eV/Å. We used the Vanderbilt ultrasoft pseudopotentials [10] and the generalized gradient approximation by Perdew and Wang (PW91) [11] for the exchange-correlation energy.

The optimized geometries for monomer, dimer, and bilayer on Pt(111) are schematically shown in Fig. 1 and further specified in Table I. For monomer [Fig. 1(a)], the adsorption on the top site is much more favored than the bridge or hollow sites. Water lies nearly flatly on the surface with the polar axis making an angle of 77° from the surface normal. The molecule can rotate freely in the azimuthal angle without any noticeable barrier. For the dimer case [Fig. 1(b)], both molecules prefer atop sites, forming a structure similar to the free dimer except that the unhydrogen-bonded OH of the donor molecule is lying down to the surface. The O-O distance, 2.69 Å, is much shorter than that of a free dimer, 2.86 Å (our calculation), suggesting that the H bond is strengthened upon adsorption. From Table I, one expects that the H-bond energy in the adsorbed dimer is at least $E_{\text{ads}}[\text{dimer}] - E_{\text{ads}}[\text{monomer}] \times 2 = (422 - 291) \times 2 =$

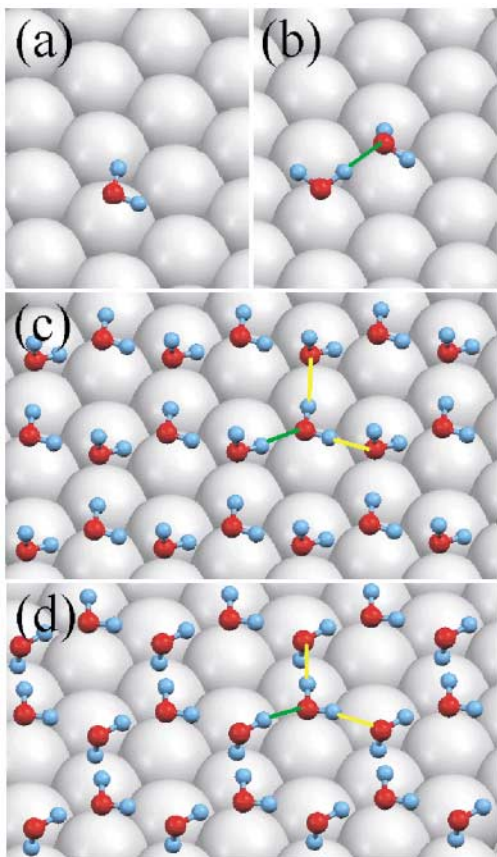


FIG. 1 (color). Equilibrium structure of (a) water monomer, (b) dimer, (c) H-up bilayer, and (d) H-down bilayer on the Pt(111) surface. The red, blue, and gray balls represent O, H, and Pt atoms, respectively. The green and yellow lines denote the two different hydrogen bonds in the bilayer.

262 meV, larger than that of the free dimer, 250 meV, as given by our calculation (experimental 236 ± 30 meV [12]). The mixing between the lone pairs of the lower O atom and the 5d bands of Pt [13], which causes electron transfer and thus an increased dipole moment, may be responsible for the enhancement of the H bond.

The lower panels [(c) and (d)] of Fig. 1 show the bilayer structure in a $\sqrt{3} \times \sqrt{3}$ surface unit cell with two waters in each cell. The waters form a puckered hexagonal network as in the bulk ice [14], with the unhydrogen-bonded

H atom pointing either upwards [H-up case, Fig. 1(c)] or to the surface [H-down case, Fig. 1(d)]. These two structures are nearly degenerate in energy, 522 (H-up) and 534 meV (H-down) (see Table I) with a barrier of 76 meV going from the H-up to H-down case. Both can be a candidate for the bilayer structure at the Pt(111) surface. For comparison, we also calculated the half-dissociated bilayer (last row of Table I) as found for Ru(0001) by Feibelman [6]. The adsorption energy is 291 meV, much lower than that of the bilayer. Therefore, dissociation is not favored on the Pt surface. The molecular bilayer was earlier suggested by ultraviolet photoemission spectroscopy [15] and low energy electron diffraction (LEED) measurement [3,16]. Our results support these experiments.

To further establish these structures, we calculated the vibrational spectra for the bilayer as shown in Fig. 2. These spectra were obtained from the velocity autocorrelation function recorded in *ab initio* MD simulation. Both the H-up (upper panel) and H-down bilayer (lower panel) are simulated. The trajectories with constant energy runs have been calculated for 2 ps, with a time step of 0.5 fs, at ~ 90 K. The left side of the spectra are a sharp peak at 4 (6) meV and five additional modes at 18 (16), 32 (34), 53 (57), 69 (69), and 87 (91) meV. (The numbers in the parentheses are for the H-down case). Similar vibrational peaks at 16.5, 33, 54, 65, and 84 meV have been observed in the HREELS spectra [16] (see Table II). They have been assigned to the Pt-OH₂ vertical vibrations for the top H₂O (32 meV) and the bottom (16 meV) molecule, and the frustrated rotations and/or librational modes (54, 69, 87 meV). The Pt-OH₂ vibrations were usually believed to be around 68 meV [17,18]. Recent experiments by Jacobi *et al.* [16] pointed out that these modes should correspond to the strong energy loss at 16.5 and 33 meV. Our MD simulations support the new assignment. The sharp peak at 4 (6) meV is close to the measured data, 5.85 meV, for the frustrated translation mode of the bilayer as observed in the He atom scattering (HAS) [19]. Modes at higher energies are related to intramolecular motions, i.e., the HOH bending mode at 198 meV and the OH stretch modes in the 380 ~ 470 meV region. From Fig. 2 and Table II, it is obvious that the calculated vibrational frequencies for the bilayer, either H-up or H-down

TABLE I. The geometry and energetics for water monomer, dimer, and bilayer adsorbed on Pt(111). Z_{OO} , Z_{OPt_1} and Z_{OPt_2} are the vertical distances between the top and bottom O atoms, the bottom O, and the underlying Pt, and the top O and the Pt, respectively.

	Z_{OO} (Å)	Z_{OPt_1} (Å)	Z_{OPt_2} (Å)	E_{ads} (meV/molecule)
Monomer	...	2.43	...	291
Dimer	0.68	2.30	3.05	422
Bilayer (H-up)	0.63	2.70	3.37	522
Bilayer (H-down)	0.35	2.68	3.14	534
Half-dissociated	0.06	2.12	2.23	291

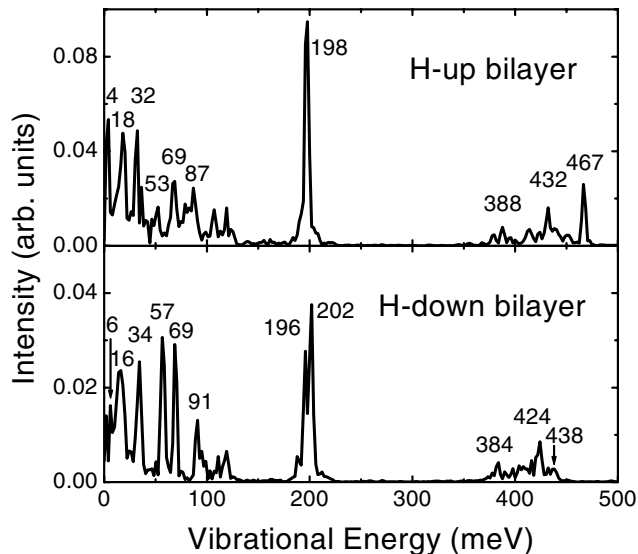


FIG. 2. Vibrational spectra for the H-up (up panel) and H-down (low panel) bilayer on Pt(111).

case, agree well with the experimental data. Although we cannot, at this stage, distinguish the two structures from the vibrational spectra.

What is more interesting are the OH modes on the right side of the spectra. These modes are sensitive to intermolecular interaction, in particular, to the H-bond formation. In Fig. 2, three modes at 388 (384), 432 (424), and 467 (438) meV are discernible. Compared to the OH frequencies, 454 meV (symmetric) and 466 meV (asymmetric) [12] in the gas phase, we may assign the high frequency mode in Fig. 2 to the unhydrogen-bonded OH mode, and the two lower modes, 388 (384) and 432 (424) meV, to the OH stretch within the bilayer. The latter are red shifted substantially, due to the H-bond formation. These modes reflect directly the structure of the bilayer. As shown in Fig. 1, the top H_2O donates 1 H atoms while the bottom molecule donates 2 H atoms in order to form a single (the green line in Fig. 1) and double H bonds (the yellow lines) with the neighboring molecules. The single bond therefore is much stronger, resulting in larger redshift, while the double H bonds are relatively weaker and thus smaller redshift.

TABLE II. Vibrational energies for the H-up and H-down bilayer on Pt(111) (in unit of meV). See the text and Ref. [16] for the assignment of these modes.

	$T_{ }$	T_2	T_3	L_3	L_4	L_5	δ_{HOH}	$\nu_{\text{O-Hb}}$	$\nu_{\text{O-H}}$
H-up	4	18	32	53	69	87	198	388, 432	467
H-down	6	16	34	57	69	91	196, 202	384, 424	438
Expt. ^a	5.85 ^b	16.5	33	54	65	84	201	424	455

^aReference [16] except for the peak at 5.85 meV.

^bReference [19].

This interpretation can be justified by tracing the trajectories of the OH bonds in the time domain as shown in Fig. 3, where the vibrational amplitudes for all four OH bonds were plotted as a function of time for the H-up bilayer. The upper panel shows the free OH bond and the strong H bond. The free OH has the shortest bond length and highest frequency, while the strong H-bonded OH has the lowest frequencies but largest bond length. The lower panel shows the two weak H-bonded OH, which lie in between the two cases in the upper panel. The vibrationally averaged bond lengths are 0.973, 0.987, and 1.000 Å for the free, weak H-bonded and strong H-bonded OH. Fourier transform of the curves in Fig. 3 yield frequencies close to 467, 432, and 388 meV, confirming the vibrational assignment given above. Figures 2 and 3 clearly show the sensitivity of OH vibrations to the H-bond formation in the bilayer. We believe that it may serve as a promising way for the recognition of the H-bonded network in general.

Comparing to experiments, modes at 424 and 455 meV are observed in the HREELS spectra [16]. They correspond to the two modes on the right side of Fig. 2. Other experiments also found a peak in the 360 ~ 400 meV region [1]. This peak was, however, previously assigned to the OH-Pt vibration against the surface [20]. The strong H-bonded peak was not discernible in the HREELS for H_2O on Pt(111) [17], but was resolved in the infrared reflection adsorption spectroscopy of D_2O on Pt(111) [20]. In the latter case, a broad peak at 2200 cm^{-1} was observed and corresponds to $\sim 3000 \text{ cm}^{-1}$ (370 meV) for $\text{H}_2\text{O}/\text{Pt}$ after scaling with the isotope factor 1.35. It is comparable to the strong H-bonded OH at 384 (388) meV. The OH frequencies in

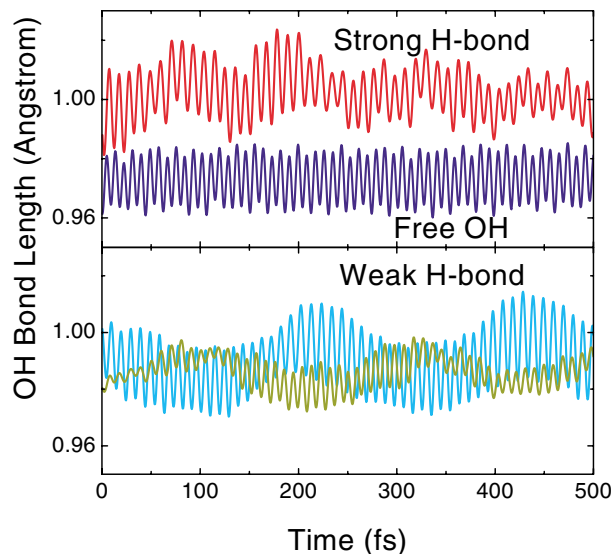


FIG. 3 (color). The variation of OH bond length versus time recorded in a 500 fs MD simulation for the H-up bilayer on Pt(111).

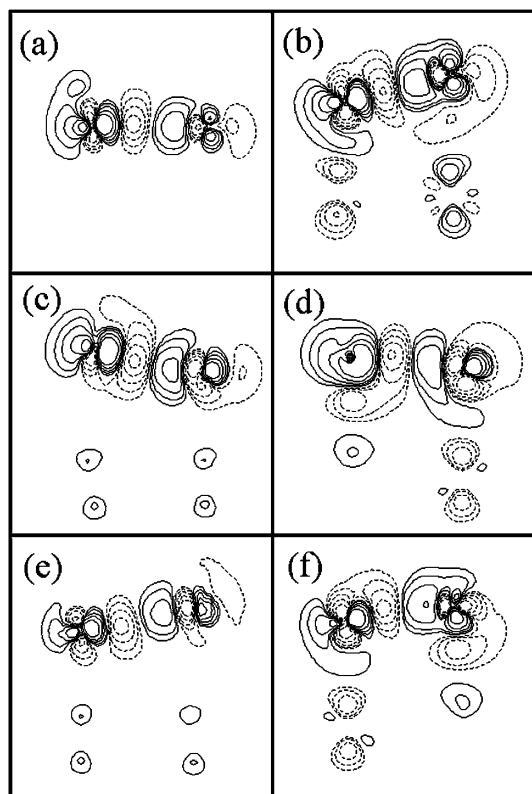


FIG. 4. Isodensity contours for the difference electron density for (a) the free water dimer, (b) the adsorbed dimer on Pt(111), (c) the strong H bond in the H-up bilayer, (d) the strong H bond in the H-down bilayer, (e) the weak H bond in the H-down bilayer, and (f) the weak H bond in the H-down bilayer. The difference density is defined as $\Delta\rho = \rho[(\text{H}_2\text{O})_2] - \rho[\text{H}_2\text{O}_{(1)}] - \rho[\text{H}_2\text{O}_{(2)}]$ for a free dimer and $\Delta\rho = \rho[2(\text{H}_2\text{O})/\text{Pt}] - \rho[\text{H}_2\text{O}_{(1)}/\text{Pt}] - \rho[\text{H}_2\text{O}_{(2)}/\text{Pt}] + \rho[\text{Pt}]$ for the other cases. The contours have densities $\Delta\rho = \pm 0.005 \times 2^n e/\text{\AA}^3$, for $n = 0, 1, 2, 3, 4$. Solid and dashed lines correspond to $\Delta\rho > 0$ and $\Delta\rho < 0$, respectively.

Fig. 2 also compare favorably with the OH modes, 390 and 403 meV, in Ice Ih [1]. By this, all the vibrational features of the bilayer have been identified and characterized.

The two types of H bonds, recognized from the vibrational spectra, have their physical origin in the bonding nature at the surface. Figure 4 shows the charge redistribution caused by H-bond formation for a free water dimer [Fig. 4(a)], adsorbed dimer [Fig. 4(b)], and water bilayers [Figs. 4(c)–4(f)]. The horizontal axis goes through the O–H–O bond while the vertical one lies in the surface normal. For the free dimer [Fig. 4(a)], formation of the H bond leads to electron transfer from the proton donor (the dashed lines on the left molecule) to the acceptor in the bonding region. This charge redistribution is greatly enhanced in the adsorbed dimer [Fig. 4(b)], indicating that the H bond is strengthened in the adsorbed phase as found in the energetics. For the strong H bond in

the bilayer [H-up case in Fig. 4(c) and H-down in Fig. 4(d)], the charge redistribution is very similar to that of the adsorbed dimer. However, the charge redistribution is less significant for the weak H bonds [Fig. 4(e) and 4(f)] in the bottom water. This difference confirms once again our findings that the H bonds in the bilayer are of two types: one strong H bond plus two weak H bonds. The enhancement of H bond upon adsorption is dramatically different from the usual picture of adsorbate-adsorbate interaction, which should, according to Pauling's principle, be reduced when they make bonds with other atoms at the surfaces. Whether this feature is unique to water or general to other H-bonded systems and what are the physical origin for such an unusual behavior need further investigations.

This work was partly supported by the National Science Foundation, the National Key Project for Basic Research (G2000067103), and the National Key Project for High-Tech (2002AA311150) of China. S. Gao was supported by The Swedish Research Council (VR) through Grant No. VR 621-2001-2614, and the Materials Consortium-ATOMICS, funded by the Swedish Foundation for Strategic Research (SSF).

- [1] P. A. Thiel and T. E. Madey, *Surf. Sci. Rep.* **7**, 211 (1987); M. A. Henderson, *Surf. Sci. Rep.* **46**, 1 (2002).
- [2] M. Odellius, M. Bernasconi, and M. Parrinello, *Phys. Rev. Lett.* **78**, 2855 (1997).
- [3] M. Morgenstern, T. Michely, and G. Comsa, *Phys. Rev. Lett.* **77**, 703 (1996); M. Morgenstern *et al.*, *Z. Phys. Chem.* **198**, 43 (1997).
- [4] A. Glebov *et al.*, *J. Chem. Phys.* **106**, 9382 (1997).
- [5] G. Held and D. Menzel, *Phys. Rev. Lett.* **74**, 4221 (1995).
- [6] P. J. Feibelman, *Science* **295**, 99 (2002); D. Menzel, *Science* **295**, 58 (2002).
- [7] G. Kresse and J. Hafner, *Phys. Rev. B* **47**, 558 (1993); **49**, 14251 (1994); G. Kresse and J. Furthmüller, *Comput. Mater. Sci.* **6**, 15 (1996); *Phys. Rev. B* **54**, 11169 (1996).
- [8] H. J. Monkhorst and J. D. Pack, *Phys. Rev. B* **13**, 5188 (1976).
- [9] M. Methfessel and A. T. Paxton, *Phys. Rev. B* **40**, 3616 (1989).
- [10] D. Vanderbilt, *Phys. Rev. B* **41**, 7892 (1990).
- [11] J. P. Perdew *et al.*, *Phys. Rev. B* **46**, 6671 (1992).
- [12] F. Sim *et al.*, *J. Am. Chem. Soc.* **114**, 4391 (1992).
- [13] H. P. Bonzel, G. Pirug, and J. E. Müller, *Phys. Rev. Lett.* **58**, 2138 (1987).
- [14] D. L. Doering and T. E. Madey, *Surf. Sci.* **123**, 305 (1982).
- [15] G. B. Fisher and J. L. Gland, *Surf. Sci.* **94**, 446 (1980).
- [16] K. Jacobi *et al.*, *Surf. Sci.* **472**, 9 (2001).
- [17] F. T. Wagner and T. E. Moylan, *Surf. Sci.* **191**, 121 (1987).
- [18] B. A. Sexton, *Surf. Sci.* **94**, 435 (1980).
- [19] A. L. Glebov, A. P. Graham, and A. Menzel, *Surf. Sci.* **427**, 22 (1999).
- [20] H. Ogasawara, J. Yoshinobu, and M. Kawai, *J. Chem. Phys.* **111**, 7003 (1999).